ADVANCED MATERIALS
www.advmat.de

Fatigue-Resistant Polymer Electrolyte Membranes for Fuel Cells

Minju Kim, Guogao Zhang, Segeun Jang, Sanghyeok Lee, Zhigang Suo, and Sang Moon Kim**

In a hydrogen fuel cell, an electrolyte membrane conducts protons, but blocks electrons, hydrogen molecules, and oxygen molecules. The fuel cell often runs unsteadily, resulting in fluctuating water production, causing the membrane to swell and contract. The cyclic deformation can cause fatigue crack growth. This paper describes an approach to develop a fatigue-resistant polymer electrolyte membrane. The membrane is prepared by forming an interpenetrating network of a plastic electrolyte and a rubber. The former conducts protons, and the latter enhances fatigue resistance. The introduction of the rubber modestly reduces electrochemical performance, but significantly increases fatigue threshold and lifespan. Compared to pristine plastic electrolyte, Nafion, an interpenetrating network of Nafion and perfluoropolyether (PFPE) reduces the maximum power density by 20%, but increases the fatigue threshold by 175%. Under the wet/dry accelerated stress test, the fuel cell with the Nafion-PFPE membrane has a lifespan 1.7 times that of a fuel cell with the Nafion membrane.

1. Introduction

In a hydrogen fuel cell, an anode and a cathode are separated by a polymer electrolyte membrane, which is a proton conductor and an electron insulator. At the anode, hydrogen molecules decompose into electrons and protons. The electrons transport through an external metal wire to the cathode, and the protons transport through the polymer electrolyte membrane to the cathode. At the cathode, the electrons, protons, and oxygen molecules react to form water, which swells the membrane. As a vehicle accelerates and decelerates, the fuel cell runs unsteadily, causing the membrane to swell and contract.[1–3] In addition to protons, hydrogen molecules can also cross over the membrane and react with oxygen molecules to form water, as well as hydrogen peroxide, hydroxyl radicals, and other radicals. The radicals can break the polymer chains in the membrane.[4–7] The combination of cyclic deformation and radical attacks can initiate and grow fatigue cracks in the membrane.[8,9] The cracks and the radicals exacerbate each other: the cracks allow more hydrogen crossover and generate more radicals, which in turn grow more cracks. The concurrent crack growth and radical attacks limit the lifetime of the fuel cell. Radical attacks can be alleviated by adding radical scavengers.[8,10] Also, hydrocarbon electrolyte membranes are less permeable to hydrogen crossover.[11–13] These approaches retard radical attacks, but do not always prevent fatigue crack growth. Particle-reinforced membranes can enhance modulus and strength, but have not shown to enhance fatigue resistance.[14–16]

Here we present a class of membranes that improve fatigue resistance. Such a membrane is composed of an interpenetrating network consisting of Nafion and perfluoropolyether (PFPE). Nafion is a widely used plastic electrolyte, while PFPE forms a rubbery polymer network. Our experiments indicate that Nafion has a fatigue threshold below 100 J m^{-2}, whereas our composite membrane has a fatigue threshold above 250 J m^{-2}. In addition, we conduct a wet/dry accelerated stress test, following a protocol established by the Department of Energy of the United States. This test reveals that the Nafion membrane has a lifespan of 242 h, while the composite membrane has a lifespan of 410 h. Compared to pristine plastic electrolyte, Nafion, an interpenetrating network of Nafion and PFPE reduces the maximum power density by 20%. These findings together indicate the introduction of the rubbery network modestly lowers electrochemical performance, but significantly enhances fatigue resistance and overall lifespan. It is hoped that this work contributes to the development of durable fuel cells.

2. Results and Discussion

We prepare the composite electrolyte membrane as follows. We start with a commonly used plastic electrolyte membrane, Nafion

M. Kim, S. M. Kim
Department of Mechanical Engineering
Incheon National University
Incheon 22012, Republic of Korea
E-mail: ksm7852@inu.ac.kr
G. Zhang, Z. Suo
John A. Paulson School of Engineering and Applied Sciences
Harvard University
Cambridge, MA 02138, USA
E-mail: suo@seas.harvard.edu
S. Jang, S. Lee
School of Mechanical Engineering
Kookmin University
Seoul 02707, Republic of Korea

The ORCID identification number(s) for the author(s) of this article can be found under https://doi.org/10.1002/adma.202308288

DOI: 10.1002/adma.202308288

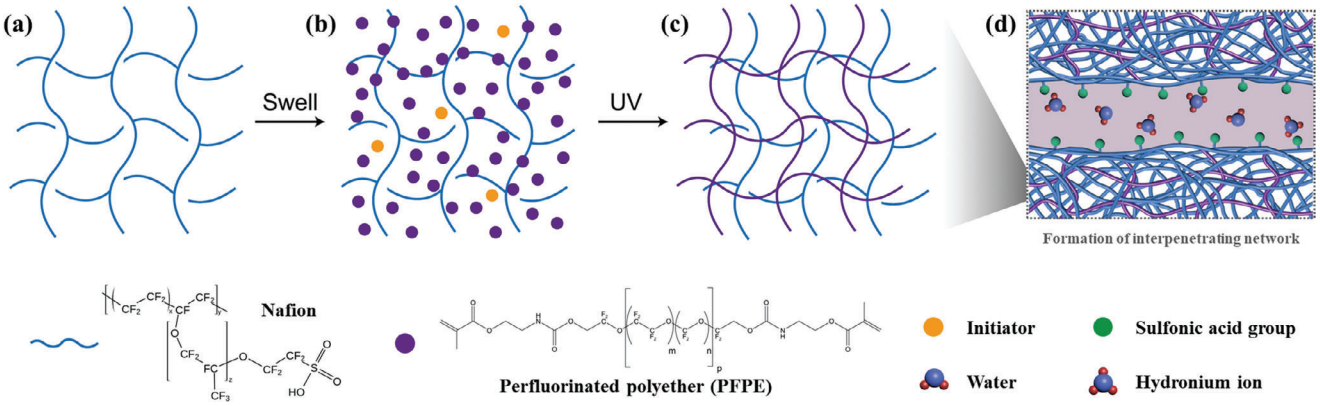

Figure 1. The preparation of the composite electrolyte membrane. a) Schematic of a Nafion membrane structure. b) Nafion membrane is swollen in the PFPE precursor. c) Through UV curing, PFPE and Nafion form an interpenetrating polymer network. d) The composite membrane contains interpenetrating network of PFPE and polytetrafluoroethylene backbones, and ion-conducting channels.

(**Figure 1a**). Nafion consists of polytetrafluoroethylene (PTFE) backbones, which have randomly tethered side chains with sulfonic acid groups ($SO_3^-H^+$).[15,17] Consequently, the polymer chains of Nafion are amphiphilic: the PTFE backbones are hydrophobic, but the sulfonic acid groups are hydrophilic.[18] In contact with water, Nafion forms continuous hydrophobic domains and continuous hydrated channels. The former provides mechanical support, and the latter transports protons as hydronium ions (H_3O^+). We choose PFPE as a second component to fulfill several requirements. First, the precursor should be hydrophobic and able to diffuse into Nafion. Second, after curing, the polymers should form an interpenetrating network with Nafion. Third, in contact with water, the polymer should have minimum interference with the hydrated channels. Fourth, the polymer network should be rubbery, so that the PFPE can deconcentrate stress at a crack tip in the interpenetrating network. Fifth, it is required to ensure the chemical stability of the material in consideration of the harsh operating conditions of fuel cells. (see details of Fenton's test and Figure S1, Supporting Information) Considering these requirements, we use a well-known PFPE-based material: perfluoropolyether-urethane dimethacrylate mixed with a photoinitiator. We submerge Nafion in the liquid precursor of PFPE. The hydrophobic precursor diffuses into the backbones of Nafion (Figure 1b). We then UV-cure the precursor to form an interpenetrating polymer network of Nafion and PFPE (Figure 1c). The PFPE chains are hydrophobic and form an interpenetrating polymer network with PTFE backbones, with minimum interference with the hydrated channels (Figure 1d).

We measure the swelling ratio, w/w_i as a function of time, where w is the weight of the membrane containing absorbed precursor, w_i is the initial weight of the membrane (**Figure 2a**). The film saturates at $w/w_i = 1.217$ after ≈70 h, and reaches 50% of saturation at 6 h. We prepare composite membranes of 50% of saturation (Nafion-PFPE-50) and 100% saturation (Nafion-PFPE-100). The solid content of Nafion in the composite membrane after swelling in PFPE precursor can be simply obtained by taking the reciprocal of the swelling ratio. The solid contents of Nafion in the composite membrane were 90.2% and 82.2% for Nafion-PFPE-50 and Nafion-PFPE-100, respectively. To homogenize the precursor, each membrane is kept in the ambient conditions for a day before UV curing. We conduct uniaxial tensile tests for Nafion, pristine PFPE film, Nafion-PFPE-50, and Nafion-PFPE-100 (Figure 2b). Young's modulus and tensile strength are 144 and 10.23 MPa for Nafion, 27.11 and 5.79 MPa for pristine PFPE film, 65.67 and 5.46 MPa for Nafion-PFPE-50, and 56.45 and 4.98 MPa for Nafion-PFPE-100. We also stretch samples with precut crack to measure toughness, G_c (Figure 2c). The elastic energy density function $w(\lambda)$ is calculated by integrating the stress–stretch curve until stretch λ. The sample with a crack is then monotonically stretched until rupture, and the stretch λ_c when the crack starts to propagate is recorded. The toughness is calculated as $w(\lambda_c)\cdot H$, where H is the height of the sample. The toughness is calculated as the area under the curve of the uncut sample between stretch 1 and λ_c, where λ_c is the stretch when the crack starts to propagate in the precut sample. The toughnesses are 16.04, 3.19, 7.81, and 5.28 kJ m^{-2} for Nafion, pristine PFPE film, Nafion-PFPE-50, and Nafion-PFPE-100 (Figure 2d). We observe the surfaces of the samples using scanning electron microscopy (SEM) (Figure S2, Supporting Information). The surface of Nafion-PFPE-50 seems to be comparable to that of the Nafion, which indicates that the interpenetrating network forms inside of the membrane and not at the surface. However, Nafion-PFPE-100 forms craze, likely due to excessive the PFPE precursor on the surface.

We prepare precut samples, pull them cyclically (**Figure 3a**), and record the crack growth per cycle (Figure 3b). Each sample is pulled from the original state $\lambda = 1$ to stretch of a fixed amplitude $\lambda_{applied}$ at a constant speed at a constant stretch rate of 12 mm min^{-1} for 10 000 cycles. The crack growth is measured to calculate the crack growth per cycle, dc/dN. The amplitude of energy release rate is calculated by

$$G = w\left(\lambda_{applied}\right)\cdot \mathrm{H} \tag{1}$$

where H is the height of the sample, and $w(\lambda_{applied})$ is the energy density in the membrane at stretch $\lambda_{applied}$. Fatigue threshold (G_0) is defined as the energy release rate below which no crack advance is observed. The fatigue threshold is 100 J m^{-2} for the NRE-212, 5.18 J m^{-2} for pristine PFPE film, 150 J m^{-2} for Nafion-PFPE-100, and 275 J m^{-2} for Nafion-PFPE-50. (Figure 3b;

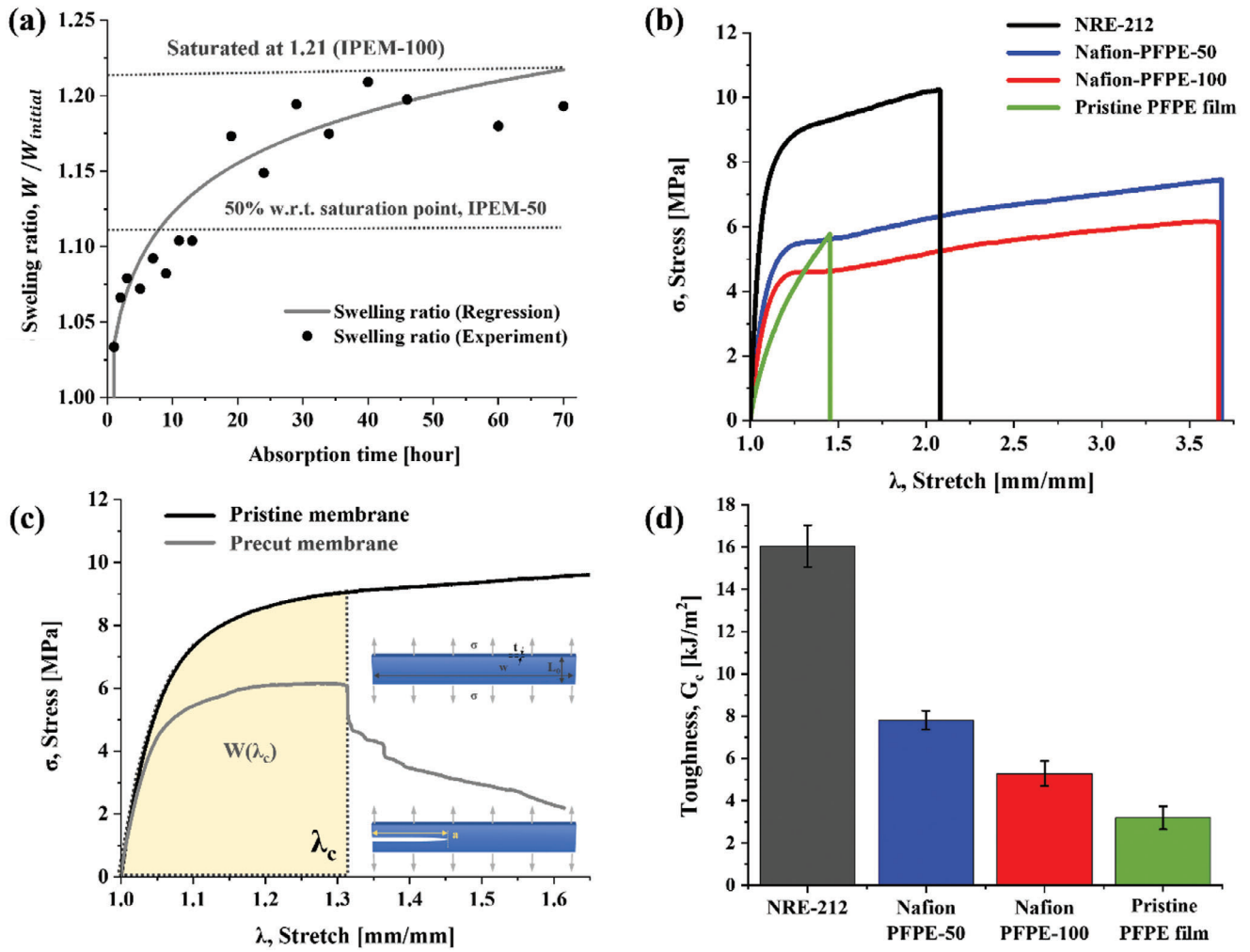

Figure 2. The preparation and mechanical properties of composite electrolyte membrane. a) Submerged in the PFPE precursor, the Nafion film absorbs the precusor, and the weight increases with time. b) The stress–stretch curve of pristine Nafion (NRE-212), pristine PFPE film, Nafion-PFPE-50 and Nafion-PFPE-100 membranes. c) A sample without precut and a sample with precut are monotonically loaded until rupture, and the stress-stretch curves are recorded. d) The toughness of NRE-212, pristine PFPE film, Nafion-PFPE-50, and Nafion-PFPE-100.

Figure S3, Supporting Information) The NRE-212 and Nafion-PFPE-50 before and after the 150 000 cycles of stretch are observed with a digital camera (Figure 3c,d). In both cases, the amplitude of the energy release rate is 200 J m^{-2}. The crack grows in the NRE-212, but not in the Nafion-PFPE-50. Also note that Nafion-PFPE-50 exhibits a significant improvement in fatigue threshold compared to Nafion-PFPE-100.

The fatigue threshold of an elastomer network has been extensively studied using the Lake-Thomas model.[19] The plastic flow of the elastomer does not contribute to the fatigue threshold. The fatigue threshold is entirely due to the breaking of the covalent polymer network. At the crack tip, right before a polymer chain breaks, the entire chain is stretched near the covalent bond strength. When the chain breaks at a single covalent bond, the energy of the entire chain is dissipated. Consequently, the fatigue threshold of the elastomer network scales with the covalent energy per unit volume times the thickness of the single layer of the polymer chain. The longer the polymer chain, the higher the fatigue threshold. There is no established theory for the fatigue threshold of a thermoplastic. The thermoplastic consists of uncrosslinked polymer chains, which slip at a shear stress order of magnitude lower than the tensile strength of a polymer chain. During cyclic loading, the polymer chain at the crack tip can be pulled out from the bulk cycle by cycle if the chains are relatively short. Alternatively, the polymer chain may break if the chain is long enough to be jammed in the bulk. When the chain breaks at the single covalent bond, the energy of a long segment of the chain is released. This shear lag model has been examined in a recent paper,[20] but has not been used to predict fatigue threshold. The fatigue threshold of a composite of elastomer network and thermoplastic has been studied experimentally recently.[21] It has been suggested that the large difference in the elastic moduli of the elastomer and thermoplastic deconcentrates stress, allowing high stress to transmit over a long length in the thermoplastic. This mechanism is proposed to account for the enhanced fatigue threshold in an elastomer-thermoplastic composite. Similar enhancement in fatigue threshold has been reported in biological tissue.[22] Upon examining the trends and outcomes of

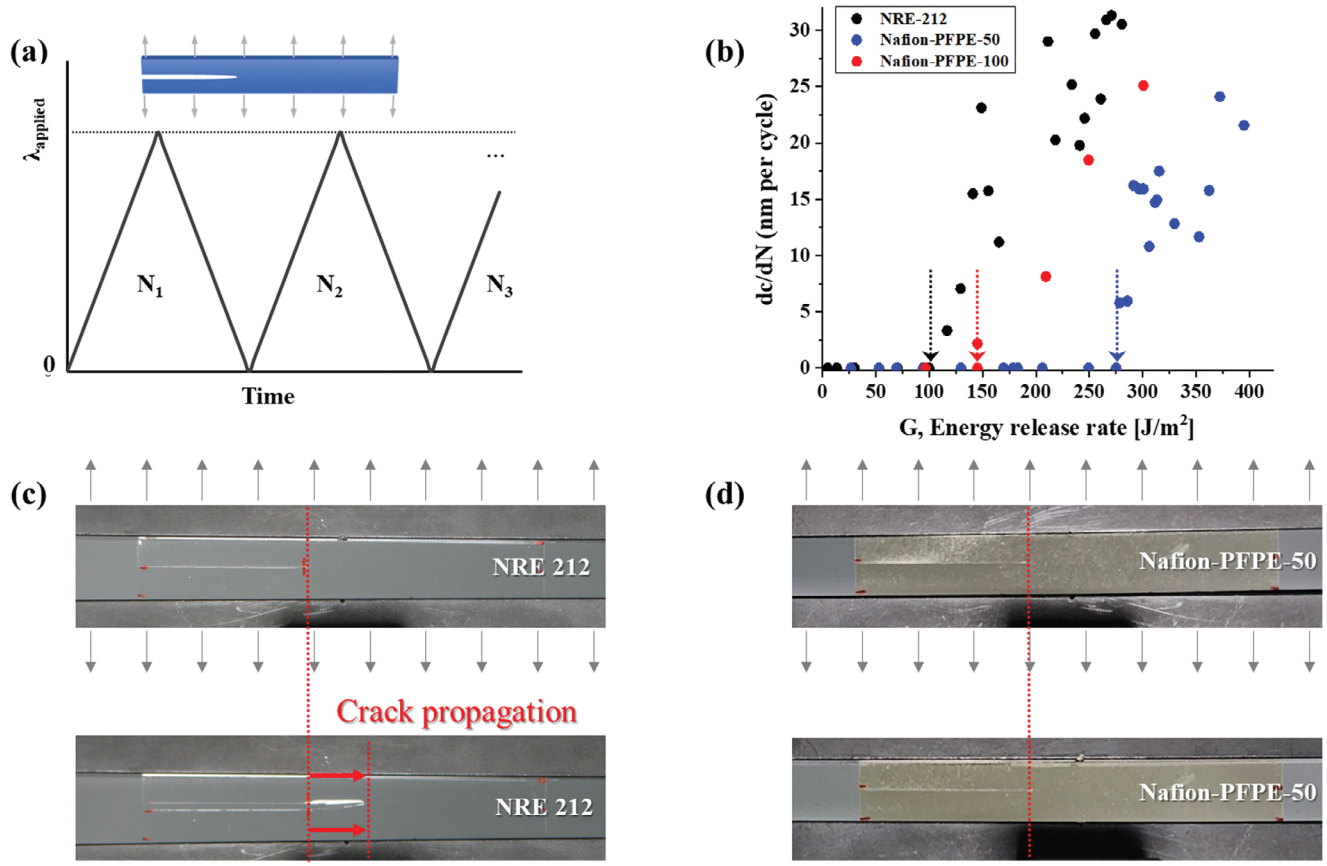

Figure 3. Fatigue test of the Nafion (NRE-212) and composite electrolyte membrane. a) A precut sample is cyclic pulled between stretch $\lambda = 1$ and a fixed stretch $\lambda_{applied}$ at a constant speed. b) Crack growth per cycle (dc/dN) is recorded as a function of the amplitude of energy release rate G. c) Optical images of Nafion before and after 150 000 cycles at an energy release rate of 200 J m^{-2}. d) Optical images of Nafion-PFPE-50 before and after fatigue test of 150 000 cycles at an energy release rate of 200 J m^{-2}.

these studies, it appears that the fatigue resistance of Nafion-PFPE-50 has been enhanced due to similar stress deconcentration effects in the aforementioned research.

We next characterize the performance of NRE-212, Nafion-PFPE-50, and Nafion-PFPE-100 in fuel cells. We sandwich a membrane between two electrodes, and connect the electrodes to a metal through a variable resistor. As protons migrate through the membrane, and electric current flows through the resistor, we measure the voltage between the two electrodes as a function of the current. Compared to NRE-212, Nafion-PFPE-100 shows a substantial decrease in current density, but Nafion-PFPE-50 shows a modest decrease in current density (**Figure** 4a). For example, at 0.6 V the current density is 0.892 A cm^{-2} for NRE-212, 0.042 A cm^{-2} for Nafion-PFPE-100, and 0.574 A cm^{-2} for Nafion-PFPE-50. A comparable trend is also observed under low RH operating conditions (Figure S4, Supporting Information).

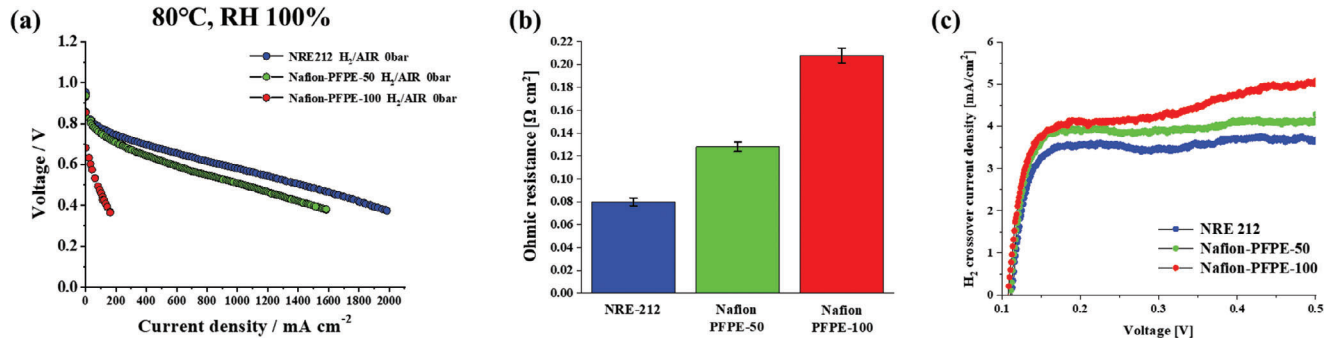

Figure 4. Electrochemical measurements of the Nafion and composite electrolyte membrane. a) Voltage–current curves of fuel cells with NRE-212, Nafion-PFPE-50, and Nafion-PFPE-100 membranes at 80 °C and RH 100%, b) A plot of measured high-frequency resistances of fuel cells with the three types of membranes. c) Hydrogen crossover current density of the membranes.

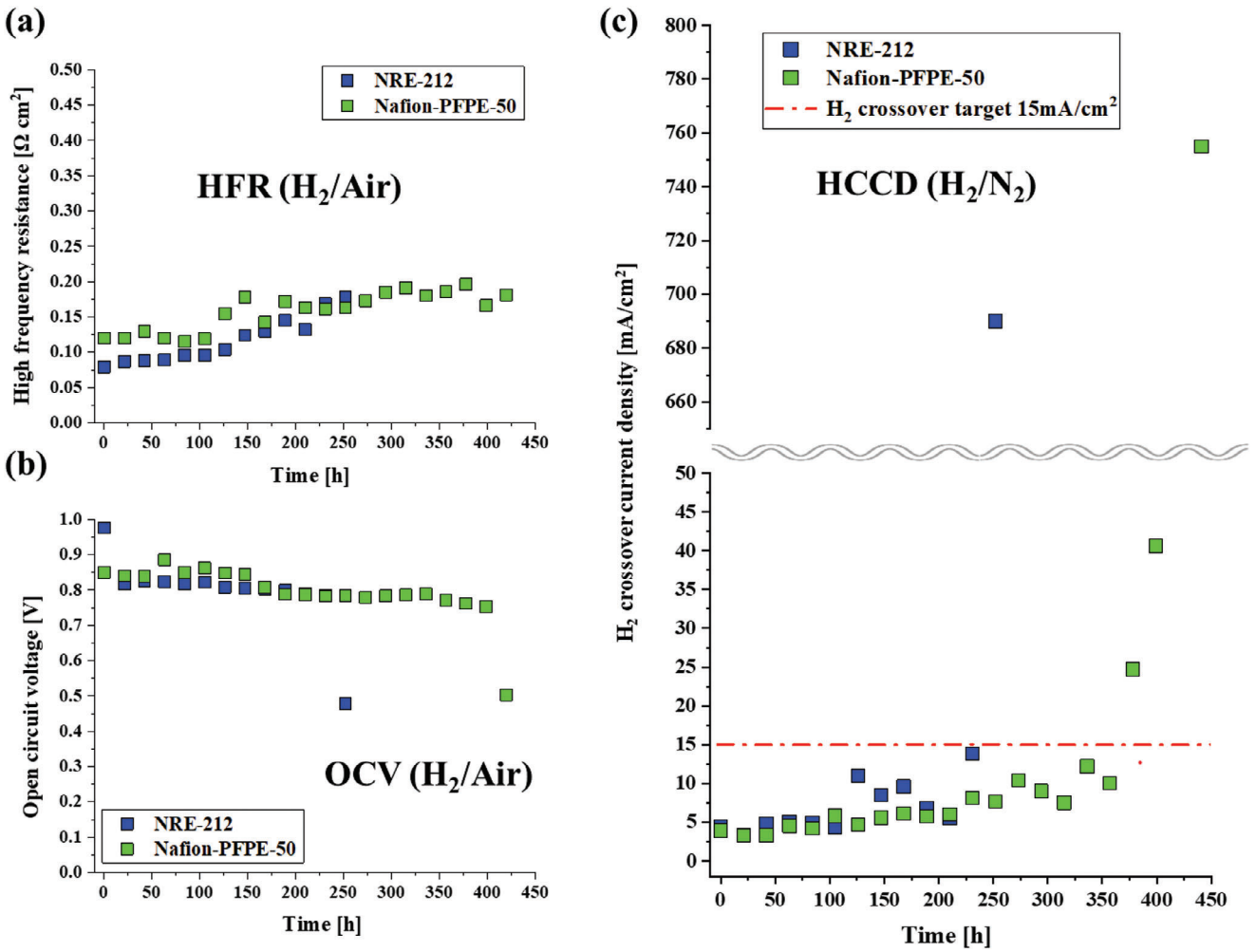

Figure 5. Variation of electrochemical performance of the Nafion and Nafion-PFPE-50 under wet/dry accelerated stress test a) High-frequency resistance. b) Open circuit voltage. c) Hydrogen crossover current density.

Investigation of oxygen reduction reaction activity is addressed in the Figures S5 and S6 (Supporting Information). We apply an alternating current in the range of 0.1–100 kHz, and measure the ohmic resistance of the three membranes (Figure 4b). The ohmic resistance is inversely proportional to the proton conductance of the membrane. And the proton conductivity, membrane resistance, and interfacial resistance for NRE-212, composite membranes are summarized in Table S1 (Supporting Information). The Nafion-PFPE-100 exhibits the highest ohmic resistance (0.208 Ω cm^2) among the experimental set, and membrane resistance of Nafion-PFPE-100 is higher by 107% compared to NRE-212, which is mainly ascribed to the blocking of the proton pathway by the excessive absorption of PFPE precursor to the Nafion membrane. In the case of Nafion-PFPE-50, the ohmic resistance is 0.128 Ω cm^2, which is comparable to that of NRE 212 (0.083 Ω cm^2). We characterize hydrogen crossover using linear sweep voltammetry[11,23,24] (Figure 4c; Figure S7, Supporting Information). Both Nafion-PFPE-50 and Nafion-PFPE-100 show a modest increase in hydrogen crossover relative to NRE-212. This increase is likely due to the increased permeability of elastomer PFPE in the membrane.

An in situ accelerated stress test is conducted to verify whether the membrane durability is improved by enhanced fatigue resistance when applied to a fuel cell system. The US Department of Energy has proposed a relative humidity cycling protocol to evaluate the durability of electrolyte membranes. The protocol repeatedly changes RH 0 for 30 s and RH 100 for 45 s in the condition of temperature of 90 °C, H_2/O_2 gas supply environment. Repetitive swelling and contraction of the membrane are induced by the cyclic change in RH, which reflects the response of the membrane to acceleration and deceleration in operating the fuel cell. The repetitive membrane deformation leads to the initiation and propagation of pinholes and cracks, which in turn accelerate hydrogen crossover. This ultimately results in operational failure of the fuel cell due to heat generation and voltage drop from gas mixing reactions.[25] The two membranes have a comparable change in ohmic resistance as a function of time (**Figure 5a**). This increase can be attributed to the increased interfacial resistance between the membrane and catalyst layer. This is supported by data showing that the interfacial resistance of Nafion-PFPE-100 exceeds that of NRE-212 by 170%, as detailed in Table S1 (Supporting Information). The open circuit voltage drops substantially at

242 h for NRE 212, and at 410 h for Nafion-PFPE-50 (Figure 5b). Similarly, hydrogen crossover increases substantially at 242 h for NRE 212, and at 368 h for Nafion-PFPE-50. (Figure 5c). And the voltage–current curves of NRE-212 and Nafion-PFPE-50 after the in situ accelerated stress test were obtained (Figure S8, Supporting Information). The current density at 0.5 V decreased by 94% for NRE-212 and 92% for Nafion-PFPE-50, indicating that the membrane had reached the end of its operational lifespan. The protocol from the department of energy identifies the substantial changes in open circuit voltage and hydrogen crossover as two indicators of lifetime. In our experiment, the two indicators suggest an enhancement of lifetime by 69% extended lifetime. When another Nafion-PFPE-50 membrane was fabricated and an identical test was performed, comparable results were obtained, confirming reproducibility. (Figure S9, Supporting Information)

3. Conclusion

We have demonstrated a fatigue-resistant electrolyte membrane based on an interpenetrating polymer network of PFPE and NRE-212. We have prepared membranes with different amounts of PFPE, designated as Nafion-PFPE-50 and Nafion-PFPE-100. Compared to the pristine Nafion membrane, Nafion-PFPE-50 increases the fatigue threshold by 175%, and Nafion-PFPE-100 increases the fatigue threshold by 50%. The membranes are characterized by voltage–current curves, ohmic resistance, and hydrogen crossover current density. The Nafion-PFPE-100 is much degraded compared to NRE-212, which is ascribed to severe blocking of the proton conducting channels by an excessive amount of PFPE. By contrast, the Nafion-PFPE-50 exhibits electrochemical properties comparable to those of NRE-212, which indicates that the interpenetrating network does not seriously block the proton-conducting channels. We have also conducted the wet/dry accelerated stress test, which measures hydrogen crossover current density and open circuit voltage as functions of time. The lifetime of the Nafion-PFPE-50 is 410 h, while the lifetime of the NRE-212 is 242 h. These findings show that the interpenetrating network enhances the fatigue resistance of the membrane and extends the lifetime of the fuel cell. It is hoped that the proposed approach can help to realize durable energy conversion and storage systems.

4. Experimental Section

Materials: Pristine Nafion membrane, NRE-212 with a thickness of ≈50 µm, was purchased from DuPont (US). The oligomer Fluorolink MD700 (perfluoropolyether-urethane dimethacrylate (PFPE)) was purchased from Solvay Solexis Inc (Italy). The photoinitiator Darocur 1173 (2-Hydroxy-2-methylpropiophenone) was purchased from Merck (Germany).

Preparation of Photo-Curable Precursor: Fluorolink MD700 and Darocur 1173 were mixed at a weight ratio of 99:1 (99 wt.% of Fluorolink MD700) in an amber vial.

Membrane Preparation: NRE-212 was submerged into the mixed PFPE precursor for a specific time. After wiping off the excess precursor on the membrane surface, the membrane impregnated with precursor was left on a clear petri dish at room temperature for a day for homogenization of the precursor in the membrane network.

Fabrication of Interpenetrating Polymer Electrolyte Membrane: The Nafion membrane impregnated with PFPE precursor was inserted into the UV curing chamber, and was irradiated with the UV light (365 nm) with an intensity of 2 mW cm^{-2} for 12 h.

Characterization of Mechanical Property: The samples were cut into 5 cm in width and 2.1 cm in height. After a sample was gripped with the rubber-coated grippers of a tensile tester (Instron 3342, USA), the remaining height of the sample was 0.7 cm. In the uniaxial strain test, the velocity was fixed at 0.05 mm min^{-1}. In the fatigue test, the membrane with precut was stretched to a specific stretch for 10 000 cycles and the velocity was fixed as 12 mm min^{-1}. After the fatigue cycling test, crack propagation of the membrane was observed by an optical microscope (Olympus BX53M, Japan). The crack propagation rate was calculated by dividing the crack growth by the number of cycles.

Preparation of Membrane Electrode Assembly and Single Cell: The catalyst ink was prepared by mixing 94 mg of carbon-supported platinum catalyst (40% Pt on Vulcan XC-72R, FC Catalyst, United States), 0.645 mL of 5 wt.% Nafion ionomer solution (Sigma–Aldrich, US), 0.376 mL of deionized water, and 9.4 mL of isopropyl alcohol (Sigma–Aldrich, US). The Nafion ionomer loading ratio, which was the weight of Nafion ionomer over the total weight of the dried mixture of Nafion and carbon-supported platinum, was 23 wt. %. The mixture was placed in a sonication bath for 30 min. The catalyst ink was sprayed onto the membranes with a platinum loading of 0.2 mg cm^{-2} on both electrodes. The samples were dried at ambient conditions for 12 h. Each of the membrane electrode assemblies with an active area of 5.0 cm^{-2} was assembled with a gas diffusion layer (SGL 39BB, SGL Carbon, Germany) and bipolar plates in a single cell.

Electrochemical Characterization: In the fully humidified operating condition, the cell was set at a temperature of 80 °C, the cathode was supplied with RH 100% air at a rate of 800 sccm, and the anode was supplied with hydrogen gas at a rate of 150 sccm. In the low-humidified condition, the cell was set at a temperature of 95 °C, the cathode was supplied with RH 55% air at a rate of 800 sccm, and the anode was supplied with hydrogen gas at a rate of 150 sccm. The high-frequency resistance of each membrane electrode assembly was measured by using an impedance analyzer (HCP-803, BioLogic, France) at a DC current of 1 A, AC amplitude of 100 mA, and frequency ranging from 0.1 to 100 kHz. The hydrogen crossover current density was measured using the linear sweep voltammetry from 0 to 0.5 V, with a scan rate of 2 mV s^{-1}. The membrane was set at a temperature of 80 °C, the cathode was supplied with nitrogen at a rate of 200 sccm, and the anode was supplied with hydrogen gas at a rate of 200 sccm. The wet/dry accelerated stress test was conducted under the temperature of 90 °C, the cathode was supplied with oxygen gas at a rate of 200 sccm, and the anode was supplied with hydrogen gas at a rate of 200 sccm. The gas pressure at the flow rate was 103.82 kPa for both sides.

Proton Conductivity of the Membranes: The proton conductivity was assessed by cutting the membranes into dimensions of 1 cm × 4 cm and placing them into the conductivity cell, where four Pt wire was positioned at a distance of 1 cm for each electrode as shown in Figure S10 (Supporting Information). To measure the membrane resistance, electrochemical impedance spectroscopy was used in the frequency range from 1 MHz to 1 Hz, with a constant current of 0.1 mA at 80 °C, while fully humidified nitrogen gas was supplied to the anode and cathode at a flow rate of 200 mL min^{-1}, respectively. The conductivity of membranes was calculated using the equation of $\sigma = L/RA$ where L, R, and A denote the distance between the electrodes, membrane resistance, and cross-sectional area of the membrane, respectively.

Supporting Information

Supporting Information is available from the Wiley Online Library or from the author.

Acknowledgements

M.K. and G.Z. contributed equally to this work. This work was supported by the National Research Foundation (NRF) of Korea (NRF-2021M3H4A1A02042957 and RS-2023-00277319). Z.S. acknowledges the

support of the Air Force Office of Scientific Research under award number FA9550-20-1-0397.

Conflict of Interest

The authors declare no conflict of interest.

Data Availability Statement

The data that support the findings of this study are available from the corresponding author upon reasonable request.

Keywords

fatigue resistant, fuel cells, interpenetrating network, perfluorinated monomer, polymer electrolyte membrane

Received: August 16, 2023
Revised: December 16, 2023
Published online:

[1] B. Wu, M. Zhao, W. Shi, W. Liu, J. Liu, D. Xing, Y. Yao, Z. Hou, P. Ming, J. Gu, Z. Zou, *Int. J. Hydrogen Energy* **2014**, *39*, 14381.
[2] J. B. Ballengee, P. N. Pintauro, *Macromolecules* **2011**, *44*, 7307.
[3] Y. Tang, A. Kusoglu, A. M. Karlsson, M. H. Santare, S. Cleghorn, W. B. Johnson, *J. Power Sources* **2008**, *175*, 817.
[4] Q. Meyer, Y. Zeng, C. Zhao, *Adv. Mater.* **2019**, *31*, 1901900.
[5] M. Hu, G. Cao, *Int. J. Hydrogen Energy* **2014**, *39*, 7940.
[6] L. Ghassemzadeh, T. J. Peckham, T. Weissbach, X. Luo, S. Holdcroft, *J. Am. Chem. Soc.* **2013**, *135*, 15923.
[7] D. E. Curtin, R. D. Lousenberg, T. J. Henry, P. C. Tangeman, M. E. Tisack, *J. Power Sources* **2004**, *131*, 41.
[8] S. Shi, X. Sun, Q. Lin, J. Chen, Y. Fu, X. Hong, C. Li, X. Guo, G. Chen, X. Chen, *Int. J. Hydrogen Energy* **2020**, *45*, 27653.
[9] Q. Lin, Z. Liu, L. Wang, X. Chen, S. Shi, *J. Power Sources* **2018**, *398*, 34.
[10] Z. Rui, J. Liu, *Prog. Nat. Sci.: Mater. Int.* **2020**, *30*, 732.
[11] C. Klose, T. Saatkamp, A. Münchinger, L. Bohn, G. Titvinidze, M. Breitwieser, K.-D. Kreuer, S. Vierrath, *Adv. Energy Mater.* **2020**, *10*, 1903995.
[12] S. H. Mirfarsi, M. J. Parnian, S. Rowshanzamir, E. Kjeang, *Int. J. Hydrogen Energy* **2022**, *47*, 13460.
[13] T. Zhang, W. He, J. Goldbach, D. Mountz, J. Yi, *J. Power Sources* **2011**, *196*, 1687.
[14] A. M. Baker, L. Wang, W. B. Johnson, A. K. Prasad, S. G. Advani, *J. Phys. Chem. C* **2014**, *118*, 26796.
[15] S. Jang, Y. S. Kang, D. Kim, S. Park, C. Seol, S. Lee, S. M. Kim, S. J. Yoo, *Adv. Mater.* **2022**, *35*, 2204902.
[16] Y.-H. Liu, B. Yi, Z.-G. Shao, D. Xing, H. Zhang, *Electrochem. Solid-State Lett.* **2006**, *9*, A356.
[17] S. Yuk, M.-J. Choo, D. Lee, H. Guim, T.-H. Kim, D. G. Lee, S. Choi, D.-H. Lee, G. Doo, Y. T. Hong, H.-T. Kim, *Adv. Mater.* **2017**, *29*, 1603056.
[18] G. Dorenbos, *Polymer* **2013**, *54*, 5024.
[19] G. Lake, A. Thomas, *Proc. R. Soc. London, Ser. A* **1967**, *300*, 108.
[20] S. Hassan, J. Kim, Z. Suo, *J Mech Phys Solids* **2022**, *158*, 104675.
[21] G. Zhang, J. Kim, S. Hassan, Z. Suo, *Proc. Natl. Acad. Sci. USA* **2022**, *119*, 2203962119.
[22] L. Zeng, F. Liu, Q. Yu, C. Jin, J. Yang, Z. Suo, J. Tang, *Sci. Adv.* **2023**, *9*, eade7375.
[23] R. Shimizu, K. Otsuji, A. Masuda, N. Sato, M. Kusakabe, A. Iiyama, K. Miyatake, M. Uchida, *J. Electrochem. Soc.* **2019**, *166*, F3105.
[24] T. Huang, X. Qiu, J. Zhang, X. Li, Y. Pei, H. Jiang, R. Yue, Y. Yin, Z. Jiang, X. Zhang, M. D. Guiver, *J. Power Sources* **2022**, *527*, 231143.
[25] F. A. De Bruijn, V. A. T. Dam, G. J. M. Janssen, *Fuel cells* **2008**, *8*, 3.